

# 1 Reference genome bias in light of species-specific 2 chromosomal reorganization and translocations

3 **Marius F. Maurstad<sup>1</sup>, Siv Nam Khang Hoff<sup>1</sup>, José Cerca<sup>1</sup>, Mark Ravinet<sup>1</sup>, Ian Bradbury<sup>2</sup>, Kjetill S.  
4 Jakobsen<sup>1</sup>, Kim Præbel<sup>3</sup>, Sissel Jentoft<sup>1</sup>**

5 <sup>1</sup>Centre for Ecological and Evolutionary Synthesis, Department of Biosciences, University of Oslo, Oslo, Norway

6 <sup>2</sup>Fisheries and Oceans Canada, Newfoundland, St John's, Canada

7 <sup>3</sup>Norwegian College of Fishery Science, The Arctic University of Norway, Tromsø, Norway

## 8 Summary

9 Whole-genome sequencing efforts has during the past decade unveiled the central role of  
10 genomic rearrangements—such as chromosomal inversions—in evolutionary processes,  
11 including local adaptation in a wide range of taxa. However, employment of reference genomes  
12 from distantly or even closely related species for mapping and the subsequent variant calling,  
13 can lead to errors and/or biases in the datasets generated for downstream analyses. Here, we  
14 capitalize on the recently generated chromosome-anchored genome assemblies for Arctic cod  
15 (*Arctogadus glacialis*), polar cod (*Boreogadus saida*), and Atlantic cod (*Gadus morhua*) to  
16 evaluate the extent and consequences of reference bias on population sequencing datasets  
17 (approx. 15-20x coverage) for both Arctic cod and polar cod. Our findings demonstrate that  
18 the choice of reference genome impacts population genetic statistics, including individual  
19 mapping depth, heterozygosity levels, and cross-species comparisons of nucleotide diversity  
20 ( $\pi$ ) and genetic divergence ( $D_{XY}$ ). Further, it became evident that using a more distantly related  
21 reference genome can lead to inaccurate detection and characterization of chromosomal  
22 inversions, i.e., in terms of size (length) and location (position), due to inter-chromosomal  
23 reorganizations between species. Additionally, we observe that several of the detected species-  
24 specific inversions were split into multiple genomic regions when mapped towards a  
25 heterospecific reference. Inaccurate identification of chromosomal rearrangements as well as  
26 biased population genetic measures could potentially lead to erroneous interpretation of  
27 species-specific genomic diversity, impede the resolution of local adaptation, and thus, impact

28 predictions of their genomic potential to respond to climatic and other environmental  
29 perturbations.

30 **Introduction**

31 Recent advancement within sequencing technologies and bioinformatic tools have  
32 revolutionized the field of biology. Pioneering studies have been conducted within human  
33 genomics, which have improved our understanding of biological processes tremendously. The  
34 number of studies on wildlife and marine species is also increasing<sup>1–4</sup>, and over the past years,  
35 several larger international initiatives have been established to characterize all of life's genomic  
36 diversity<sup>5</sup>. Within these efforts, the overall goal is to generate highly contiguous reference  
37 genomes (i.e., chromosome level) that can be used in a i) comparative setting to describe the  
38 genomic diversity between species, and/or conduct ii) within-species genome-wide  
39 characterization of cryptic ecotypes and sub-population differentiations<sup>4–7</sup>.

40 While the number of high-quality reference genomes is growing, there is still a shortage  
41 in the number of reference genomes available for various taxa<sup>8</sup>. In the cases where a reference  
42 genome for the focal species is missing, the standard method is to select a close relative for  
43 mapping and subsequent variant calling<sup>9</sup>. When using a reference genome from a distantly  
44 related species (or a divergent population), the genomic divergence between the reference and  
45 the target species can impact mapping, variant calling, and downstream inferences<sup>9–14</sup>. For  
46 instance, measures of heterozygosity—important measures for conservation genomics—can be  
47 overestimated when employing more divergent references<sup>10–13</sup>. However, few studies have  
48 examined how discrepancies in genomic architecture between the reference and target species  
49 would impact the identification of e.g., larger structural variants, such as chromosomal  
50 inversions. Since the beginning of the genomics area, chromosomal inversions have been  
51 recognized as part of the standing genomic variation of a species, and/or sub-  
52 populations/ecotypes, that are likely to play important roles in evolutionary processes,

53 including local adaptation<sup>15–20</sup>. For instance, in Atlantic cod (*Gadus morhua*; L., 1758), four  
54 larger chromosomal inversions are found to discriminate between populations throughout its  
55 geographical distribution, i.e., dominating the observed genomic divergence by large allele  
56 frequency shifts<sup>15,21–23</sup>. It is suggested that these are of high importance for maintaining the  
57 genomic divergence between locally adapted populations as well as the iconic migratory  
58 Northeast Arctic cod (NEAC) and the more stationary Norwegian coastal cod (NCC)<sup>15,21–24</sup>.  
59 Would such and other structural variants be overlooked or inadequately characterized due to  
60 larger or smaller inter-chromosomal reorganizations between the reference used and the focal  
61 species? In an earlier study conducted on European plaice (*Pleuronectes platessa*), a difference  
62 in number of putative chromosomal inversions were recorded based on using the species-  
63 specific reference vs. using the Japanese flounder (*Paralichthys olivaceus*)<sup>25,26</sup> that potentially  
64 could be due to species-specific differences in number of inversions and/or other types of inter-  
65 chromosomal reorganizations.

66 Within the gadids, major genomic reorganizations and reshufflings have been  
67 documented, and especially within the two cold-water specialists: the Arctic cod (*Arctogadus*  
68 *glacialis*; Peters, 1872) and the polar cod (*Boreogadus saida*; Lepechin, 1774)<sup>27</sup>. Additionally,  
69 for polar cod a large number of polymorphic chromosomal inversions (with the potential  
70 impact on sub-population structuring) have been detected<sup>28</sup>. Such major genomic  
71 reorganizations and reshufflings could potentially lead to downstream bioinformatic errors in  
72 mapping, variant calling, and data interpretation, depending on the selection of reference. In  
73 this study, we aimed at taking the full advantage of the newly generated chromosome-anchored  
74 genome assemblies of the closely related Arctic cod<sup>27</sup>, polar cod<sup>27</sup>, and NEAC<sup>29</sup> to assess how  
75 the selected reference genome impacts the mapping depth, heterozygosity level and measures  
76 of population differentiation and divergence between Arctic cod and polar cod, when exploring  
77 population-level data of the two species collected from the northern Barents Sea and adjacent

78 regions (Figure 1b). Additionally, we investigated how the different reference genomes  
79 influence the detection of chromosomal inversions, focusing exclusively on the Arctic cod.  
80 Both Arctic cod and polar cod represent important sympatric species inhabiting the Arctic, one  
81 of the world's most rapidly changing environments that is undergoing warming at a pace almost  
82 four times faster than the global average<sup>30</sup>. Until now, there are only a few studies that have  
83 looked into the population genetic structuring of Arctic cod and polar cod using a handful of  
84 genetic markers<sup>31–36</sup> and even fewer that have used whole genome sequencing approaches<sup>28,37</sup>,  
85 and by such, this study will advance our insight into the genomic composition and potential  
86 within these species in the light of the ongoing climatic changes.

## 87 Materials and Methods

### 88 Sample acquisition and sequencing

89 The collection of Arctic cod (N=14, Table S1) used in this study was obtained via the TUNU-  
90 cruises (UiT, The Arctic University of Norway) and from other international collaborators,  
91 including N=11 individuals from Northeast Greenland (Tyroler and Besselfjord) and N=2  
92 individuals from Canada (Davis Strait), as well as one specimen collected in the Barents Sea  
93 (Figure 1b). The collection of polar cod (N=14, Table S1) is a subset from a larger dataset<sup>28</sup>  
94 from the northern Barents Sea (Figure 1b). DNA isolation for Arctic cod was done by following  
95 the QIAGEN DNeasy Blood & Tissue kit protocol. DNA concentration measurement, library  
96 preparation, and sequencing were performed by the Norwegian Sequencing Centre. See  
97 Supplementary Sequencing Report for more information.

### 98 Study design

99 The whole genome sequencing data were used to generate three *cross-species* datasets where  
100 data from both Arctic cod (N=14) and polar cod (N=14) were included (Figure 2a), as well as  
101 three *intraspecific* datasets where we focused on the Arctic cod samples (Figure 2b). Both

102 sample collections (i.e., *cross-species* and *intraspecific*) were mapped against the reference  
103 genomes of either i) Arctic cod<sup>27</sup>, ii) polar cod<sup>27</sup>, and iii) Northeast Atlantic cod (NEAC)<sup>29</sup>,  
104 with the main purpose to assess the choice of reference on mapping depth as well as  
105 heterozygosity levels. Additionally, population genetic measures, such as nucleotide diversity  
106 ( $\pi$ ), genetic differentiation ( $F_{ST}$ ), and genetic divergence ( $D_{XY}$ ) were estimated to assess the  
107 influence of reference genome choice in a *cross-species* context. Moreover, we utilized the  
108 *intraspecific* datasets to assess the precision in detection of chromosomal inversions within  
109 Arctic cod. This was conducted by comparing the degree of overlap between the inversions  
110 detected when using either the Arctic cod (i.e. the benchmark) vs. the polar cod or the NEAC  
111 genome as a reference.

## 112 **Mapping and variant calling**

113 To obtain the six separate datasets (i.e., three VCFs for the *cross-species* analysis and three  
114 VCFs focusing on the *intraspecific* analysis) we started by trimming Illumina PE reads using  
115 Trimmomatic v0.39<sup>38</sup> with default settings. Mapping to the different references was done using  
116 the Burrows-Wheeler Alignment Tool v0.7.17<sup>39</sup> (BWA-MEM algorithm) with default settings.  
117 Alignment files for each sample were merged and sorted using SAMtools v1.9<sup>40</sup>. Duplicated  
118 reads were marked using MarkDuplicates v2.22.1<sup>41</sup>. Variant calling was performed using the  
119 Genome Analysis Toolkit (GATK) v4.2.0.0<sup>42</sup>. For this, each mapped sample was individually  
120 called into GVCFs using HaplotypeCaller. GVCFs for individual samples were then combined  
121 into the six different VCFs, as described above in the experimental design, and imported into  
122 a Genomics DataBase using GenomicsDBImport. Joint genotyping was performed using the  
123 GenotypeGVCFs tool to produce final VCFs. Single nucleotide polymorphisms (SNPs) were  
124 extracted and downsampled to 100,000 SNPs using SelectVariants to make diagnostic plots for  
125 filter parameter evaluation. Filtering was done by following the GATK hard-filtering  
126 recommendations and manually inspecting the diagnostic plots as suggested in

127 <https://speciationgenomics.github.io/>. After the initial round of filtering, we used VCFtools  
128 v0.1.16<sup>43</sup> to retain only biallelic sites (see Table S2 and S3 for filtering parameters and Table  
129 S4 for the number of SNPs after filtering). Lastly, in-depth inspection of the datasets generated  
130 was conducted using PLINK v1.9<sup>44</sup> and VCFtools v0.1.16. for detection of potential data biases  
131 (for more information see Supplementary Note 1). A summary of the workflow is shown in  
132 Figure 2.

133 **Evaluation of population structure, mapping, and variant calling based on reference used**  
134 We analyzed read depth distributions of mapped reads for Arctic cod and polar cod samples  
135 against the three references using mosdepth v0.2.4<sup>45</sup> in fast mode, with a window size of 500  
136 bp. Additionally, VCFtools v0.1.16 was used to evaluate the proportion of heterozygous sites  
137 per sample. The population genetic structure between and within the two species was  
138 investigated using PLINK v1.9 to perform a Principal Component Analysis (PCA), using both  
139 the *cross-species* and the *intraspecific* datasets.

140 For an evaluation of the genetic diversity detected within the *intraspecific* datasets, we  
141 also carried out demographic inference and estimated female effective population size ( $N_e$ ) for  
142 Arctic cod using BEAST v2.6.7<sup>46</sup> under the Bayesian skyline model<sup>47</sup>. The analysis was done  
143 twice, once only with Arctic cod samples in the present study ( $N=14$ ) and including Arctic cod  
144 ( $N=33$ ) samples sourced from NCBI (see Supplementary Note 2 for more details).  
145 Additionally, for the *cross-species* datasets,  $\pi$ ,  $F_{ST}$ <sup>48</sup>, and  $D_{XY}$  between Arctic cod and polar  
146 cod were estimated using pixy v1.2.6<sup>49</sup>, applying a window size of 10,000 bp.

#### 147 **Detection of chromosomal inversions in Arctic cod**

148 For the *intraspecific datasets* (i.e., the three intraspecific VCFs mapped to the three different  
149 reference genomes) detection of chromosomal inversions was performed using complementary  
150 approaches. The workflow is illustrated in Supplementary Figure 5. First, we used a PCA-

151 based approach following Huang et al<sup>17</sup>. This involved quantifying genetic variation within  
152 each chromosome using the R package *lostruct* in windows of 50 SNPs<sup>50</sup>. When conducting  
153 PCAs of inversions, heterokaryotypes are expected to cluster between the two homokaryotype  
154 clusters for individuals carrying alternative inversion orientations<sup>51</sup>. Thus, resulting *lostruct*  
155 plots were manually checked for regions along chromosomes where the PCA for the MDS  
156 corners displayed three distinct clusters. After detecting potential inversion regions, *VCFtools*  
157 v0.1.16 was used to extract the regions harboring the inversion signal and calculate the  
158 heterozygosity for each sample. *PLINK* v1.9 was then used to calculate a new PCA of the SNPs  
159 within this region. In the cases where the PCA displayed an inversion signal, clusters were  
160 assigned to either homokaryotypes with most individuals (common group), heterokaryotypes  
161 as the group clustering in the center (het group), or homokaryotypes with the fewest individuals  
162 (rare group). Due to the low sample count for Arctic cod, the heterozygosity distribution could  
163 not be plotted using conventional boxplots, instead we used a binning strategy implemented in  
164 the *ggplot2* function *geom\_dotplot*<sup>52</sup>.

165 Next, *F<sub>ST</sub>* and *D<sub>XY</sub>* were calculated using *pixy* v1.2.6 in windows of 10,000 bp between  
166 the rare and common groups along chromosomes to assess patterns of genetic differentiation  
167 and divergence outside and inside potential inversion regions. Lastly, patterns of linkage  
168 disequilibrium (LD) were investigated for the chromosomes that displayed potential signals of  
169 inversions. The expectation for chromosomes harboring inversions is that regions within the  
170 inversion will show high LD among all samples (when both homokaryotypes are present) but  
171 not among samples with the same inversion orientation<sup>17</sup>. As the calculation of LD in a pairwise  
172 fashion for whole chromosomes produces millions of data points, SNPs had to be down-  
173 sampled. *PLINK* v1.9 was used to remove sites with more than 0.01% missing data, and SNPs  
174 were randomly thinned down to 10% of the original count. After thinning of SNPs, *PLINK*  
175 v1.9 was used to calculate LD in a pairwise fashion for the SNPs left within the chromosome

176 of interest. Due to the high number of data points still left, the R package scattermore was used  
177 to produce the LD plots<sup>53</sup>. We used the MDS plots along the chromosomes to define the  
178 boundaries of the inversions and corroborated with the LD patterns.

179 **Synteny between the three references**

180 To investigate chromosomal rearrangements synteny analysis between the Arctic cod, polar  
181 cod, and NEAC references was done using a syntenic block analysis with McScanX<sup>54</sup>. The  
182 result of the synteny analysis was visualized on the Synvisio interactive homepage<sup>55</sup>.

183 **Results & Discussions**

184 **Genetic structure of Arctic cod and Arctic cod vs. polar cod**

185 The PCA conducted on the *intraspecific* genomic dataset revealed a separation among the  
186 Arctic cod specimens along the first principal component (PC1) axis, explaining 10.7-10.9%  
187 of the variation in the datasets depending on the reference used (Figure 3a-c). Additionally, a  
188 separation along the PC2 axis was demonstrated, explaining 8.31-8.42% of the variation in the  
189 datasets (Figure 3a-c). When inspecting this separation against the various variant calling  
190 statistics (Figure S1-S3), we found that neither mean depth nor presence of missing sites  
191 appeared to have a notable influence on the positioning of the samples within the PCA. Mean  
192 depth was generally consistent across most samples, except for a single individual from Davis  
193 Strait. This individual, sourced from a publicly available dataset (Table S1), had been  
194 sequenced to a greater depth (approx. 30x coverage) than the others. Furthermore, among the  
195 samples, one individual from Besselfjord displayed a higher degree of missing data compared  
196 to the rest. The proportion of heterozygous sites, however, tended to overlap to some degree  
197 with the sample positioning along the PC1 axis. It should be noted that this was not the case  
198 for all samples, for instance, the Davis Strait sample (with the highest coverage and highest  
199 proportion of heterozygotic sites present) was placed in the middle of the gradient (Figure S1-

200 S3). Additionally, the proportion of heterozygous sites was generally higher using either polar  
201 cod or NEAC vs. Arctic cod as reference but did not impact the placement of the samples  
202 within the PCA (Figure 3a-c; Figure S1-S3). It is therefore tempting to speculate that a sub-  
203 population structuring within Arctic cod is present. However, to fully assess this and define the  
204 different sub-populations a larger dataset with more individuals from a larger geographical  
205 range is needed.

206 The PCAs on the *cross-species* datasets uncovered a distinct clustering pattern  
207 irrespective of the reference used, where the samples clustered in accordance with their  
208 respective species (Figure 3d-f), i.e., one cluster for Arctic cod and one cluster for polar cod,  
209 respectively. Additionally, a difference in how the two species clustered along the PC2 axis  
210 was detected, with Arctic cod exhibiting minimal intraspecific variation, whereas polar cod  
211 displayed intraspecific variability along the PC2 axis (Figure 3d-f), explained by 3.75-3.81%  
212 of the variation in the datasets, depending on the reference used. Taken together, these findings  
213 indicate that polar cod has a larger standing genetic variation compared to Arctic cod, which  
214 could be linked to the difference in female  $N_e$  observed between the species (Figure S4 and  
215 Hoff et al.<sup>27</sup>) as well as documented by others<sup>37,56,57</sup>.

## 216 **Impact of reference genome on mapping and variant calling statistics**

217 For the *cross-species* datasets, the estimation of mean mapping depth uncovered a species-  
218 specific variability, which was dependent on the reference genome used. We detected highest  
219 mean depth when individual sequencing data were mapped against their intraspecific reference,  
220 while using one of the two other codfishes as the reference resulted in lower mean depth (Figure  
221 4a). Lowest mapping depth was observed using NEAC as the reference, i.e., the most distant  
222 reference with lowest sequence identity and thus, the lowest potential mappability for both the  
223 Arctic cod and polar cod datasets. Notably, the polar cod datasets displayed higher overall  
224 depth levels, irrespective of reference used, due to the fact that the polar cod samples were

sequenced in a separate batch with slightly higher coverage (see Supplementary Materials and Methods in Hoff et al.<sup>28</sup>). Moreover, the proportion of heterozygous sites estimated (Figure 4b) mirrored the patterns of mean depth observed, where the lowest number of heterozygous sites was detected when the intraspecific reference was employed (Figure 4b), while a higher proportion of heterozygous sites was detected when one of the two heterospecific codfishes was used as the reference (Figure 4b). Thus, a higher mean depth resulted in a lower proportion of heterozygote sites and vice versa. Intriguingly, the degree of heterozygosity, seemed to be less impacted when using the more distantly related NEAC as a reference. Even if having the lowest mapping depth, the heterozygosity level was not as pronounced as seen when using either Arctic cod or polar cod as the reference (Figure 4a and b). These findings could potentially be coupled to the high genomic content of short tandem repeats detected within codfishes<sup>58–60</sup> combined with the GadMor3 genome assembly being of higher quality and more contiguous compared to the Arctic cod and the polar cod genome assemblies<sup>27,29</sup>. Mapping towards these lower quality genomes would potentially result in a higher degree of erroneous mapping of reads, i.e., misalignments (especially within the repetitive regions) vs. when mapping towards the higher quality NEAC genome assembly. Accordingly, the lower quality of the Arctic cod and the polar cod genomes, i.e., with a lower resolution of the repetitive regions, combined with higher sequence identity between these two species, could easily result in higher mapping depth (as documented above), as well as a higher degree of wrongly called heterozygous sites<sup>10–14,61</sup>. It should also be noted, that our findings could be explained by the fact that NEAC is genetically more divergent vs. the two other species, resulting in lower mappability and lower number of callable sites, and thus, less heterozygote sites detected. But, based on the similar number of sites called using the different references (see Table S4), the latter explanation seems less plausible.

249 For the population genetic statistics calculated for each of the species, we discovered  
250 varying results depending on the reference used (Figure 4c-e). The average  $\pi$  estimates  
251 displayed similar overall trends regardless of the reference genome used (Figure 4c; box plots).  
252 However, when either Arctic cod or polar cod was used as a reference, the non-reference  
253 species in the *cross-species* datasets exhibited a tailing of the average  $\pi$  values (Figure 4c;  
254 points). In contrast, using NEAC as a reference, the tailing appeared less pronounced and more  
255 similar to the estimates seen for the intraspecific comparisons. Similarly, the average  
256 background  $D_{XY}$  divergence (Figure 4d) between the species was higher when Arctic cod and  
257 polar cod were used as references, while a notable decrease in genetic divergence was observed  
258 when employing NEAC as the reference. These observations combined, could probably also  
259 be linked to the difference in quality of the genome assemblies, with the NEAC having the  
260 highest quality and lower degree of misalignments and/or due to poorer mappability, as  
261 discussed above. Additionally, the employment of an equally distant relative as reference for  
262 both species, could here be an asset, i.e., not introducing any reference bias towards one of the  
263 species when performing the variant calling. Such a bias could most likely influence the genetic  
264 diversity detected between the two species, seemingly resulting in an overestimation of the  
265 genetic divergence between Arctic cod and polar cod, when compared to the results achieved  
266 when using NEAC as the reference. On the other hand, when using NEAC as the reference  
267 there might be a higher chance that the polymorphic sites and the divergence detected between  
268 the two species are located within conserved regions (where the mappability is better), which  
269 could lead to an underestimation, as observed in our comparisons (Figure 4d). Contradictory  
270 to  $\pi$  and  $D_{XY}$ , calculation of average background  $F_{ST}$  differentiation between Arctic cod and  
271 polar cod uncovered a similarly high degree of fixation between the species, irrespective of  
272 which of the three references used (Figure 4e). The rather large interspecific differentiation at  
273 the whole genome-wide level corroborates the findings from the PCA analyses (Figure 3d, e

274 and f), indicating that the reference used does not impact the variant calling to any degree to  
275 determine the global degree of differentiation between the species, when using  $F_{ST}$  and/or PCA  
276 analyses. In contrast, genetic diversity and genetic divergence, measured by  $\pi$  and  $D_{XY}$ , are  
277 seemingly more sensitive to the choice of reference used.

278 **Detection of multiple chromosomal inversions in Arctic cod**

279 For the *intraspecific* dataset when using Arctic cod as reference genome we detected six  
280 chromosomal inversions that fulfilled the criteria defined by our inversion detection protocol  
281 (Figure S5). The inversions detected were found on chromosome 1, 6, 10, 11, 13, and 14,  
282 spanning from 2 Mb to 14 Mb in size (Table 1; Figure 5; Figure S6-S10). Furthermore, we  
283 detected five additional putative inversions, i.e., regions displaying the same patterns as the  
284 other inversions, but with weaker LD signals, less clear heterozygosity distribution, and/or only  
285 2 or less individuals in the rare cluster (Table 1; Figure S11-S17). Among the putative  
286 inversions, the ones identified on chromosome 7 represented a special case where two smaller  
287 regions in the center of the chromosome exhibited inversion signals but did not share the same  
288 individuals between clusters (Figure S11 and S12), and thus, denoted as two separate putative  
289 inversions. The absence of an inversion signal in the intermediate region further supports two  
290 independent inversions (Figure S13). On chromosome 9, we detected a signal indicating a  
291 putative inversion. However, this region did not display distinct R2 values along the LD  
292 heatmap (Figure S14). Lastly, putative inversions were detected on chromosomes 3 and 15,  
293 respectively, were both fulfilled all steps for inversion detection but only had a single sample  
294 in the rare cluster (Figure S15 and S16). Additionally, for chromosome 10, we identified a  
295 region upstream of the inversion that also displayed a high degree of differentiation (Figure  
296 S17). However, this upstream region lacked the distinct PCA clusters and typical  
297 heterozygosity distribution expected for inversions (Figure S17), and therefore, was not  
298 classified as part of this inversion nor as a separate putative inversion.

299 The larger number of inversions detected in Arctic cod is comparable with the higher  
300 number of inversions detected in polar cod, where in total 20 inversions are detected<sup>28</sup>. Both  
301 species resides in freezing water temperatures, and thus it is speculated that this high number  
302 is linked to cold water adaptions<sup>27</sup>.

303 **Table 1:** Inferred chromosomal inversions for Arctic cod using the three reference genomes. First column gives  
304 chromosome (Chr) in Arctic cod and the homologous chromosome is given for the other two species. The count  
305 of individuals is given in the rare group (RC), explained variation for the first principal component (PC1), and the  
306 region used to run PCA calculations. The grey coloring indicates the inversion split in two, while orange coloring  
307 denotes inversion not detected. Location on the chromosome(s) is given as Region (in Mbp).

Arctic cod				Polar cod				NEAC			
Chr	RC	PC1	Region	Chr	RC	PC1	Region	Chr	RC	PC1	Region
1	2	43.7%	42-50	15+	2	44.4%	13-18	18	2	53.4%	8-14
1	-	-	-	15+	2	40.8%	6-8	-	-	-	-
3*	1	30.5%	3-8	18*	1	45.2%	4-6	19*	1	38.3%	7-10
6	4	56.3%	45-47	5	4	44.6%	8-12	17	1	42.5%	1-5
7*	1	41.4%	20-23	3*	1	31.3%	51-54	15*	1	45.1%	18-20
7*	2	44.5%	30-32	16	-	-	-	21*	2	37.9%	17-19
9*	2	23.15%	20-25	6	2	15%	20-23	4*	2	15.3%	22-27
10	2	42%	14-23	7	2	29.8%	8-15	12	2	38.7%	1-6
11	3	26.5%	10-24	8	3	26.4%	4-15	7	3	25.4%	14-29
13	3	29.5%	1-7	14+	3	17.7%	start-1	5	3	25.7%	1-4
13	-	-	-	14+	3	13.9%	9-13	-	-	-	-
14	3	42%	22-end	10	3	48.2%	21-end	10	3	43.2%	23-27
15*	1	42.4%	7-12	12*	1	27.2%	start-3	2*	1	31.7%	16-20

308 \*Putative inversion, +split in multiple regions.

## 309 **Reference bias in inversion detection coupled to interspecific chromosomal reshufflings** 310 **and translocations**

311 By taking full advantage of the *intraspecific* datasets, we uncovered that the precision, in terms  
312 of size and location, of the inversion scoring became problematic when using a different  
313 reference genome than the focal species (Table 1). Employing NEAC as the reference genome,  
314 all six validated inversions were confirmed as well as the putative inversions (Figure S18-S28).  
315 Even though all the inversions were detected, the majority of the inversions identified were not  
316 found to be of similar size and nor with the same chromosomal positioning as the corresponding

317 inversions detected using Arctic cod as the reference. This differentiation is mainly due to the  
318 larger species-specific genomic rearrangements and translocations that have occurred within  
319 this lineage (Figure 6, 7 and Hoff et al.<sup>27</sup>). However, for some of the inversions a partly  
320 overlapping positioning was detected when inspecting homologous chromosomes, i.e., the  
321 inversions on chromosome 4, 7, 10, and 19 in NEAC vs. chromosome 9, 11, 14 and 3 in Arctic  
322 cod (Table 1). Moreover, two of the inversions detected (on chromosome 7 and 17) in NEAC  
323 were found to be larger than the corresponding inversions detected in Arctic cod (on  
324 chromosome 11 and 6). Since it has been shown for these two regions that Atlantic cod has  
325 overlapping inversions with Arctic cod<sup>27</sup>, this could imply that the signal of the Atlantic cod  
326 inversion could interfere with the detection of the true Arctic cod inversion.

327 When applying the more closely related polar cod as the reference, all inversions were  
328 detected except one of the putative inversions (Table 1; Figure S29-S41), i.e., the second  
329 inversion on chromosome 7 in Arctic cod (corresponding to chromosome 16 in polar cod;  
330 Figure S29). Also here, the majority of the inversions identified were not found to be of similar  
331 size and nor with the same chromosomal positioning as the corresponding inversions detected  
332 using Arctic cod (nor the NEAC) as reference. Moreover, for the inversion detected on  
333 chromosome 1 in Arctic cod, the inversion appeared as two separate but linked inversions, a  
334 result of chromosomal rearrangements between polar cod and Arctic cod (Figure 6c and d;  
335 Figures S30 and S31). Similarly, inaccurate identification due to intraspecific chromosomal  
336 translocations (between all three species) is seen for the region harbouring the inversion on  
337 chromosome 13 in Arctic cod (Figure 7). When employing the polar cod genome as the  
338 reference, we find that the inversion is split into two separate inversions, with no clear LD  
339 signals as well as a less clear heterozygosity distribution (Figure 7c and d; Figure S38 and 39).  
340 For the same region using NEAC as reference (Figure 6e; Figure S26), we capture the expected  
341 heterozygosity distribution, however only weak LD signals were detected. Adding to the

342 complexity of inversion detection when utilizing a more distantly related reference, the putative  
343 inversion on chromosome 3 in Arctic cod showed a much clearer LD signal when either NEAC  
344 (Figure S19) or polar cod (Figure S32) was employed.

345 **Concluding remarks**

346 Our findings combined, strongly indicate that caution must be exercised when using a  
347 heterospecific reference genome for variant calling as well as inversion scoring. The quality of  
348 the reference used as well as degree of genomic divergence between the focal species and the  
349 reference seemingly impact the variants called due to i) a lower degree of mappability and thus,  
350 losing informative genetic variation, ii) potential misalignments which could lead to f. ex. a  
351 bias towards higher degree of heterozygosity and more noisy datasets, where in-depth analyses  
352 on e.g., demography history and detection of signals of selection are highly likely to be  
353 erroneous/inflated by this type of reference bias<sup>10–14,61</sup>. Specifically, the general population  
354 genetic statistics in terms of heterozygosity, ROH, and genetic diversity, are all metrics that are  
355 often used within conservation genomics as measurements for the health situation of a species  
356 and/or populations, by estimating the standing genetic variation and thus, their adaptive  
357 capacity<sup>4,10,12,62</sup>. Our study shows that some of these metrics are seemingly more sensitive,  
358 such as  $D_{XY}$  and  $\pi$ , while the  $F_{ST}$  estimates are more robust, at least for detecting differentiation  
359 between species. However, it could be that  $F_{ST}$  estimates may be impacted if looking into  
360 differentiation within a species, i.e., between populations and/or ecotypes.

361 Most importantly, we discovered that the use of reference impacted the detection and  
362 characterization of chromosomal inversions. Important information on size, position, and  
363 linkage between regions can easily be lost due to species-specific genomic rearrangements and  
364 smaller translocations<sup>27</sup>. For instance, when using the more closely related species—the polar  
365 cod—as the reference for the detection of inversions in Arctic cod resulted in the detection of  
366 several inversions that were defined as two inversions instead of one continuous larger

367 inversion as well one inversion that was not discovered at all. This mismatch in detection of  
368 inversions is highly linked to the larger genomic reshufflings that have occurred after Arctic  
369 cod and polar cod branched off from their common codfish ancestor ~4 million years ago<sup>24</sup>.  
370 Moreover, most of the inversions detected were smaller than when using the focal species as  
371 the reference, i.e., meaning that the breakpoint regions are not fully characterized when using  
372 a non-conspecific reference. Additionally, we also uncovered that the precision of detection  
373 was impacted if the reference has inversions in the same regions as the focal species. When  
374 applying Atlantic cod as the reference, two of the inversions were found to be longer than  
375 expected, which could be explained by the fact that Atlantic cod in these regions harbor species-  
376 specific but overlapping polymorphic inversions with Arctic cod<sup>21,22,27</sup>. We speculate that  
377 highly variable breakpoint regions<sup>63,64</sup> could lead to higher degree of misalignments in these  
378 regions. Taken together, inference of detection of chromosomal inversions when using a non-  
379 conspecific reference, should be handled with care. Especially, since the breakpoint regions—  
380 where important genes under selection tend to be positioned<sup>27,65–68</sup>—seems to be lost in the  
381 scoring of the inversions, as well as the number and interlinking of inversions may be  
382 incomplete.

### 383 **Author contributions**

384 S.J., S.N.K.H., M.F.M. conceptualized the study. S.N.K.H., M.F.M. did DNA extractions.  
385 M.F.M. handled, processed, and analyzed the data. M.R. provided scripts. S.J., S.N.K.H.  
386 sampled polar cod and the single specimen of Arctic cod from the Barents Sea. I.B. and K.P.  
387 provided Arctic cod specimens from Canada and Greenland, respectively. Funding acquisition  
388 by S.J., K.P. and K.S.J.. S.J., S.N.K.H., and M.F.M. did the interpretation and discussion of  
389 results. Visualization and design of figures by S.N.K.H., M.F.M., and S.J. J.C. provided early  
390 feedback and comments to the manuscript. M.F.M. and S.J. wrote the original manuscript,

391 S.N.K.H. contributed with relevant sections and feedback. All co-authors read, provided  
392 feedback, and improved the manuscript.

393 **Data availability**

394 All unpublished raw sequences from the Arctic cod dataset will be deposited in the European  
395 Nucleotide Archive (ENA) at EMBL-EBI upon publication.

396 **Acknowledgements**

397 Library preparations and sequencing were performed by the Norwegian Sequencing Centre,  
398 Oslo. The computations were performed on resources provided by Sigma2; the National  
399 Infrastructure for High Performance Computing and Data Storage in Norway. We thank  
400 Alexandra Viertler for the codfish illustrations. We thank the crews of RV Kronprins Haakon  
401 (i.e., the Nansen Legacy project) and RV Helmer Hanssen (i.e., the TUNU-cruises) for  
402 facilitating the trawling and sample acquisition in the rough Barents Sea and in Northeast  
403 Greenland. M.F.M. would like to thank the Nansen Legacy for the early career opportunities  
404 provided to him.

405 **Funding**

406 This work was funded by the Research Council of Norway through the following  
407 projects: '**Nansen Legacy**' (RCN no. 276730) and '**Comparacod**' (RCN no. 222378).

408

409

410

411

412

413 **References**

- 414 1. Hohenlohe, P. A., Funk, W. C. & Rajora, O. P. Population genomics for wildlife  
415 conservation and management. *Mol. Ecol.* **30**, 62–82 (2021).
- 416 2. Lancaster, L. T. *et al.* Understanding climate change response in the age of genomics. *J.*  
417 *Anim. Ecol.* **91**, 1056–1063 (2022).
- 418 3. Bernatchez, L., Ferchaud, A.-L., Berger, C. S., Venney, C. J. & Xuereb, A. Genomics for  
419 monitoring and understanding species responses to global climate change. *Nat. Rev. Genet.*  
420 **25**, 165–183 (2024).
- 421 4. Andersson, L. *et al.* How fish population genomics can promote sustainable fisheries: a road  
422 map. *Annu. Rev. Anim. Biosci.* **12**, 1–20 (2024).
- 423 5. Formenti, G. *et al.* The era of reference genomes in conservation genomics. *Trends Ecol.*  
424 *Evol.* **37**, 197–202 (2022).
- 425 6. Pettersson, M. E. *et al.* A chromosome-level assembly of the Atlantic herring genome—  
426 detection of a supergene and other signals of selection. *Genome Res.* **29**, 1919–1928  
427 (2019).
- 428 7. Theissinger, K. *et al.* How genomics can help biodiversity conservation. *Trends Genet.* **39**,  
429 545–559 (2023).
- 430 8. Hotaling, S., Kelley, J. L. & Frandsen, P. B. Toward a genome sequence for every animal:  
431 Where are we now? *Proc. Natl Acad. Sci. USA.* **118**, e2109019118 (2021).
- 432 9. Bentley, B. P. & Armstrong, E. E. Good from far, but far from good: the impact of a  
433 reference genome on evolutionary inference. *Mol. Ecol. Resour.* **22**, 12–14 (2022).
- 434 10. Armstrong, E. E. *et al.* Long live the king: chromosome-level assembly of the lion  
435 (*Panthera leo*) using linked-read, Hi-C, and long-read data. *BMC Biol.* **18**, 3 (2020).
- 436 11. Gopalakrishnan, S. *et al.* The wolf reference genome sequence (*Canis lupus lupus*) and its  
437 implications for *Canis* spp. population genomics. *BMC Genomics* **18**, 495 (2017).
- 438 12. Prasad, A., Lorenzen, E. D. & Westbury, M. V. Evaluating the role of reference-genome  
439 phylogenetic distance on evolutionary inference. *Mol. Ecol. Resour.* **22**, 45–55 (2022).
- 440 13. Thorburn, D.-M. J. *et al.* Origin matters: Using a local reference genome improves  
441 measures in population genomics. *Mol. Ecol. Resour.* **23**, 1706–1723 (2023).
- 442 14. Deng, X.-L. *et al.* The impact of sequencing depth and relatedness of the reference genome  
443 in population genomic studies: A case study with two caddisfly species (Trichoptera,  
444 Rhyacophilidae, *Himalopsyche*). *Ecol. Evol.* **12**, e9583 (2022).
- 445 15. Barth, J. M. I. *et al.* Genome architecture enables local adaptation of Atlantic cod despite  
446 high connectivity. *Mol. Ecol.* **26**, 4452–4466 (2017).
- 447 16. Wellenreuther, M. & Bernatchez, L. Eco-evolutionary genomics of chromosomal  
448 inversions. *Trends Ecol. Evol.* **33**, 427–440 (2018).
- 449 17. Huang, K., Andrew, R. L., Owens, G. L., Ostevik, K. L. & Rieseberg, L. H. Multiple  
450 chromosomal inversions contribute to adaptive divergence of a dune sunflower ecotype.  
451 *Mol. Ecol.* **29**, 2535–2549 (2020).

452 18. Akopyan, M. *et al.* Comparative linkage mapping uncovers recombination suppression  
453 across massive chromosomal inversions associated with local adaptation in Atlantic  
454 silversides. *Mol. Ecol.* **31**, 3323–3341 (2022).

455 19. Merot, C. *et al.* Locally adaptive inversions modulate genetic variation at different  
456 geographic scales in a seaweed fly. *Mol. Biol. Evol.* **38**, 3953–3971 (2021).

457 20. Hager, E. R. *et al.* A chromosomal inversion contributes to divergence in multiple traits  
458 between deer mouse ecotypes. *Science* **377**, 399–405 (2022).

459 21. Berg, P. R. *et al.* Three chromosomal rearrangements promote genomic divergence  
460 between migratory and stationary ecotypes of Atlantic cod. *Sci. Rep.* **6**, 23246 (2016).

461 22. Berg, P. R. *et al.* Trans-oceanic genomic divergence of Atlantic cod ecotypes is associated  
462 with large inversions. *Heredity* **119**, 418–428 (2017).

463 23. Sodeland, M. *et al.* “Islands of divergence” in the atlantic cod genome represent  
464 polymorphic chromosomal rearrangements. *Mol. Biol. Evol.* **8**, 1012–1022 (2016).

465 24. Matschiner, M. *et al.* Supergene origin and maintenance in Atlantic cod. *Nat. Ecol. Evol.*  
466 **6**, 469–481 (2022).

467 25. Weist, P. *et al.* The role of genomic signatures of directional selection and demographic  
468 history in the population structure of a marine teleost with high gene flow. *Ecol. Evol.* **12**,  
469 e9602 (2022).

470 26. Le Moan, A., Bekkevold, D. & Hemmer-Hansen, J. Evolution at two time frames: ancient  
471 structural variants involved in post-glacial divergence of the European plaice (*Pleuronectes*  
472 *platessa*). *Heredity* **126**, 668–683 (2021).

473 27. Siv N.K Hoff *et al.* Chromosomal fusions and large-scale inversions are key features for  
474 adaptation in Arctic codfish species (Submitted). *Manuscript* (2024).

475 28. Siv N.K Hoff *et al.* Population divergence manifested by genomic rearrangements in a  
476 keystone Arctic species with high gene flow (Submitted). *Manuscript* (2024).

477 29. Jentoft, S. *et al.* The genome sequence of the Atlantic cod, *Gadus morhua* (Linnaeus, 1758).  
478 *Wellcome Open Res.* **9**, 189 (2024). <https://doi.org/10.12688/wellcomeopenres.21122.1>

479 30. Rantanen, M. *et al.* The Arctic has warmed nearly four times faster than the globe since  
480 1979. *Commun. Earth. Environ.* **3**, 1–10 (2022).

481 31. Gordeeva, N. V. & Mishin, A. V. Population Genetic Diversity of Arctic Cod (*Boreogadus*  
482 *saida*) of Russian Arctic Seas. *J. Ichthyol.* **59**, 246–254 (2019).

483 32. Madsen, M. L., Nelson, R. J., Fevolden, S.-E., Christiansen, J. S. & Præbel, K. Population  
484 genetic analysis of Euro-Arctic polar cod *Boreogadus saida* suggests fjord and oceanic  
485 structuring. *Polar Biol.* **39**, 969–980 (2016).

486 33. Maes, S. M. *et al.* High gene flow in polar cod (*Boreogadus saida*) from West-Svalbard  
487 and the Eurasian Basin. *J. Fish Biol.* **99**, 49–60 (2021).

488 34. Nelson, R. J. *et al.* Circumpolar genetic population structure of polar cod, *Boreogadus*  
489 *saida*. *Polar Biol.* **43**, 951–961 (2020).

490 35. Quintela, M. *et al.* Distinct genetic clustering in the weakly differentiated polar cod,  
491 *Boreogadus saida* Lepechin, 1774 from East Siberian Sea to Svalbard. *Polar Biol.* **44**,  
492 1711–1724 (2021).

493 36. Wilson, R. E. *et al.* Micro-geographic population genetic structure within Arctic cod  
494 (Boreogadus saida) in Beaufort Sea of Alaska. *ICES J. Mar. Sci.* **76**, 1713–1721 (2019).

495 37. Wilson, R. E. *et al.* Low levels of hybridization between sympatric cold-water-adapted  
496 Arctic cod and Polar cod in the Beaufort Sea confirm genetic distinctiveness. *Arc. Sci.* **8**(4):  
497 1082-1093. (2022) doi:10.1139/as-2021-0030.

498 38. Bolger, A. M., Lohse, M. & Usadel, B. Trimmomatic: a flexible trimmer for Illumina  
499 sequence data. *Bioinformatics* **30**, 2114–2120 (2014).

500 39. Li, H. Aligning sequence reads, clone sequences and assembly contigs with BWA-MEM.  
501 Preprint at <https://doi.org/10.48550/arXiv.1303.3997> (2013).

502 40. Danecek, P. *et al.* Twelve years of SAMtools and BCFtools. *GigaScience* **10**, giab008  
503 (2021).

504 41. Broad Institute. Picard Toolkit. *Broad Institute, GitHub repository*  
505 <https://broadinstitute.github.io/picard/> (2019).

506 42. DePristo, M. A. *et al.* A framework for variation discovery and genotyping using next-  
507 generation DNA sequencing data. *Nat. Genet.* **43**, 491–498 (2011).

508 43. Danecek, P. *et al.* The variant call format and VCFtools. *Bioinformatics* **27**, 2156–2158  
509 (2011).

510 44. Purcell, S. *et al.* PLINK: A tool set for whole-genome association and population-based  
511 linkage analyses. *Am. J. Hum. Genet.* **81**, 559–575 (2007).

512 45. Pedersen, B. S. & Quinlan, A. R. Mosdepth: quick coverage calculation for genomes and  
513 exomes. *Bioinformatics* **34**, 867–868 (2018).

514 46. Bouckaert, R. *et al.* BEAST 2.5: An advanced software platform for Bayesian evolutionary  
515 analysis. *PLoS Comput. Biol.* **15**, e1006650 (2019).

516 47. Drummond, A. J., Rambaut, A., Shapiro, B. & Pybus, O. G. Bayesian coalescent Inference  
517 of past population dynamics from molecular sequences. *Mol. Biol. Evol.* **22**, 1185–1192  
518 (2005).

519 48. Weir, B. S. & Cockerham, C. C. Estimating F-Statistics for the analysis of population  
520 structure. *Evolution* **38**, 1358–1370 (1984).

521 49. Korunes, K. L. & Samuk, K. pixy: Unbiased estimation of nucleotide diversity and  
522 divergence in the presence of missing data. *Mol. Ecol. Resour.* **21**, 1359–1368 (2021).

523 50. Li, H. & Ralph, P. Local PCA shows how the effect of population structure differs along  
524 the genome. *Genetics* **211**, 289–304 (2019).

525 51. Mérot, C. Making the most of population genomic data to understand the importance of  
526 chromosomal inversions for adaptation and speciation. *Mol. Ecol.* **29**, 2513–2516 (2020).

527 52. Wickham, H. *et al.* *ggplot2*. Springer-Verlag New York <https://ggplot2.tidyverse.org>  
528 (2016).

529 53. Kratochvíl, M., Bednárek, D., Sieger, T., Fišer, K. & Vondrášek, J. ShinySOM: graphical  
530 SOM-based analysis of single-cell cytometry data. *Bioinformatics* **36**, 3288–3289 (2020).

531 54. Wang, Y. *et al.* MCScanX: a toolkit for detection and evolutionary analysis of gene synteny  
532 and collinearity. *Nucleic Acids Res.* **40**, e49 (2012).

533 55. Bandi, V. *et al.* Visualization tools for genomic conservation. in *Plant Bioinformatics: Methods and Protocols* (ed. Edwards, D.) 285–308 (Springer US, New York, NY, 2022). doi:10.1007/978-1-0716-2067-0\_16.

536 56. Wilson, R. E. *et al.* Mitochondrial genome diversity and population mitogenomics of polar  
537 cod (*Boreogadus saida*) and Arctic dwelling gadoids. *Polar Biol.* **43**, 979–994 (2020).

538 57. Pálsson, S., Källman, T., Paulsen, J. & Árnason, E. An assessment of mitochondrial  
539 variation in Arctic gadoids. *Polar Biol.* **32**, 471–479 (2009).

540 58. Tørresen, O. K. *et al.* An improved genome assembly uncovers prolific tandem repeats in  
541 Atlantic cod. *BMC Genomics* **18**, 95 (2017).

542 59. Tørresen, O. K. *et al.* Genomic architecture of haddock (*Melanogrammus aeglefinus*)  
543 shows expansions of innate immune genes and short tandem repeats. *BMC Genomics* **19**,  
544 240 (2018).

545 60. Reinar, W. B. *et al.* Teleost genomic repeat landscapes in light of diversification rates and  
546 ecology. *Mobile DNA* **14**, 14 (2023).

547 61. Chen, N.-C., Solomon, B., Mun, T., Iyer, S. & Langmead, B. Reference flow: reducing  
548 reference bias using multiple population genomes. *Genome Biol.* **22**, 8 (2021).

549 62. Barrett, R. D. H. & Schluter, D. Adaptation from standing genetic variation. *Trends Ecol.  
550 Evol.* **23**, 38–44 (2008).

551 63. Araya, R. A. *et al.* Tandem accumulation of transposable element-derived repeats in  
552 inversion breakpoints. In prep. (2024).

553 64. Han, F. *et al.* Ecological adaptation in Atlantic herring is associated with large shifts in  
554 allele frequencies at hundreds of loci. *eLife* **9**, e61076 (2020).

555 65. Stewart, N. B. & Rogers, R. L. Chromosomal rearrangements as a source of new gene  
556 formation in *Drosophila yakuba*. *PLoS Genet.* **15**, e1008314 (2019).

557 66. Jones, F. C. *et al.* The genomic basis of adaptive evolution in threespine sticklebacks.  
558 *Nature* **484**, 55–61 (2012).

559 67. Guillén, Y. & Ruiz, A. Gene alterations at *Drosophila* inversion breakpoints provide prima  
560 facie evidence for natural selection as an explanation for rapid chromosomal evolution.  
561 *BMC Genomics* **13**, 53 (2012).

562 68. Villoutreix, R. *et al.* Inversion breakpoints and the evolution of supergenes. *Mol. Ecol.* **30**,  
563 2738–2755 (2021).

564 69. Mecklenburg, C. W. *et al.* *Marine Fishes of the Arctic Region Volume 1. Conservation of  
565 Arctic Flora and Fauna Monitoring Series 28*, Norwegian Ministry of Foreign Affairs  
566 (2018).

567

568

569

570

571

572 **Figures**

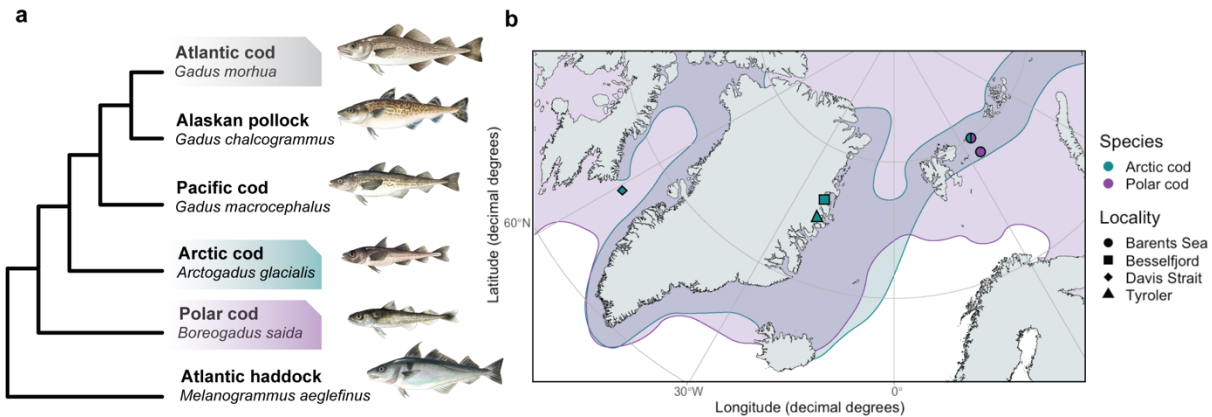
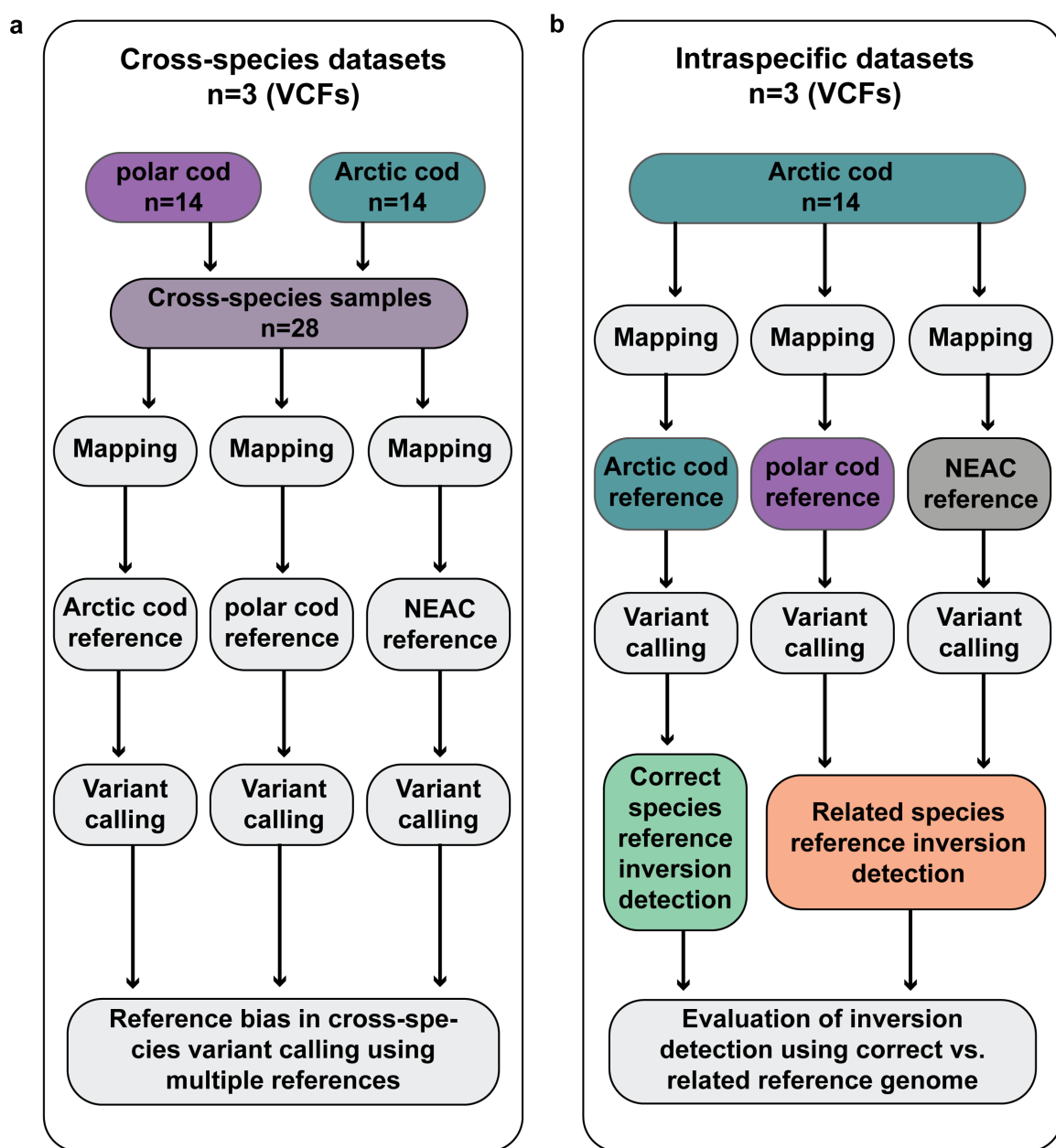
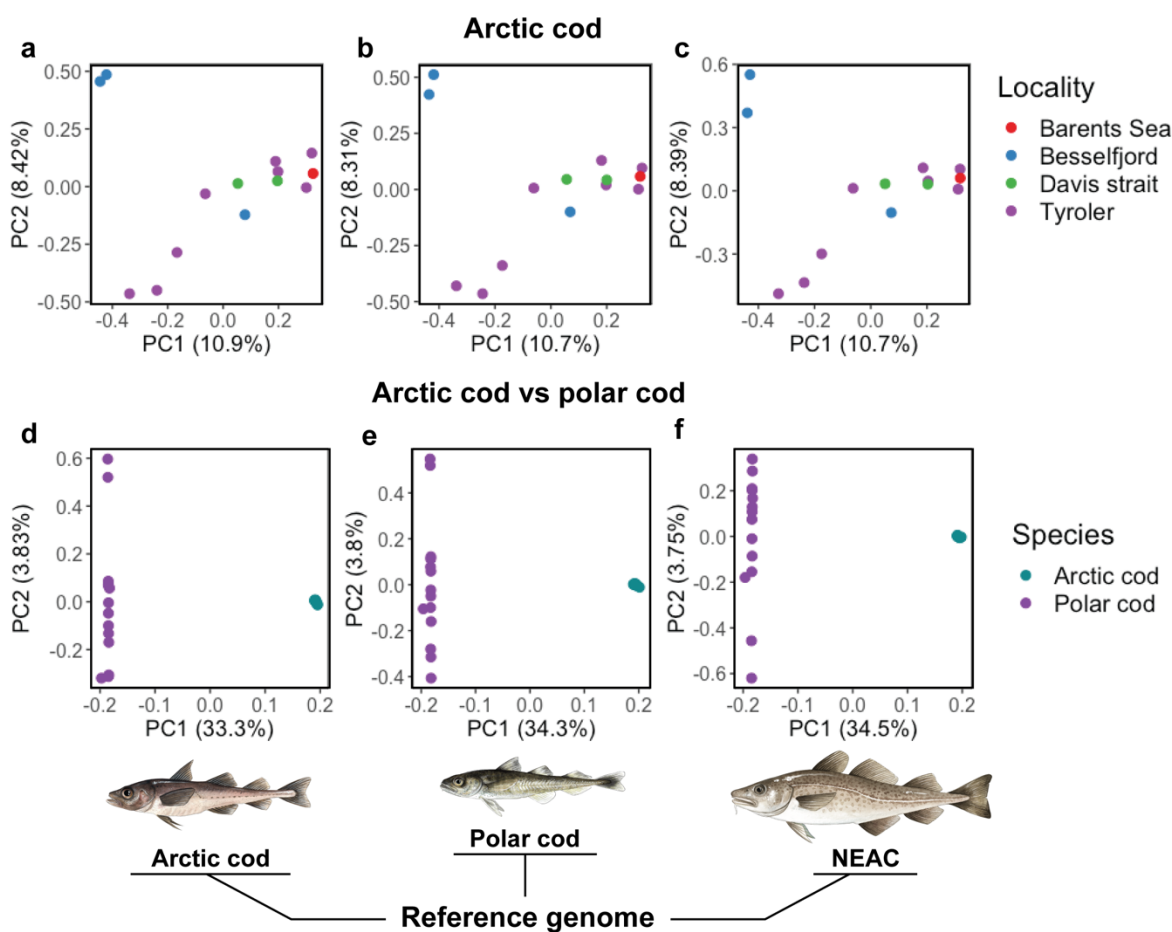


**Figure 1:** Phylogenetic relationship and distribution of Arctic cod and polar cod. a) Phylogenetic relationship of Arctic cod redrawn from Matschiner et al.<sup>24</sup> and Hoff et al.<sup>27</sup> The phylogenetic placement of Arctic cod is not fully resolved, as it may be either a sister lineage to *Gadus* or a sister species to polar cod<sup>24,27</sup>. Species used as reference genomes in this study are highlighted. b) Map of sampling localities of Arctic cod and polar cod with their distributions in the sampling region redrawn from Mecklenburg et al.<sup>69</sup> Illustrations by Alexandra Vierler.



580  
581  
582  
583  
584  
585  
586  
587  
588  
589  
590  
591  
592  
593

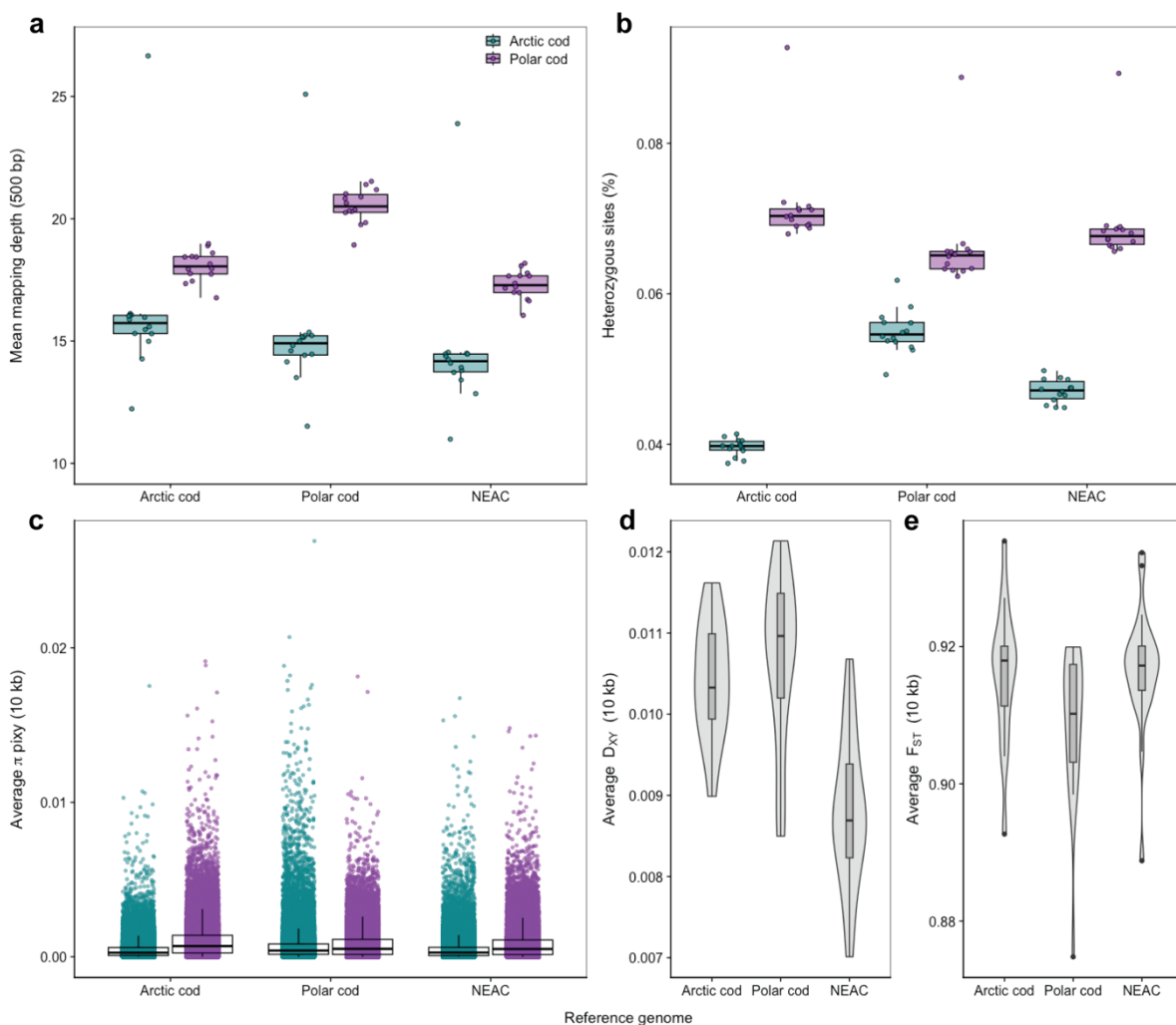
**Figure 2:** Flowchart of the sample design and generation of the *cross-species* and *intraspecific* datasets. a) For the generation of the three *cross-species* VCFs, we used samples of Arctic cod (N=14) and polar cod (N=14). Each sample was individually mapped against three different reference genomes: Arctic cod, polar cod, and (Northeast Arctic cod) NEAC. After mapping, the samples were grouped based on the reference genome they were mapped against. This approach was employed to assess the extent of reference bias in *cross-species* variant calling when using different reference genomes. b) To investigate the impact of reference bias on inversion detection, we generated three *intraspecific* datasets focusing on Arctic cod samples (N=14). These samples were mapped against the same three reference genomes used for the *cross-species* VCFs. In this analysis, the Arctic cod reference was considered the accurate benchmark for detecting inversions. The detected inversions were then compared to those identified when using a related species' reference genome, to evaluate the influence of reference choice on inversion detection.



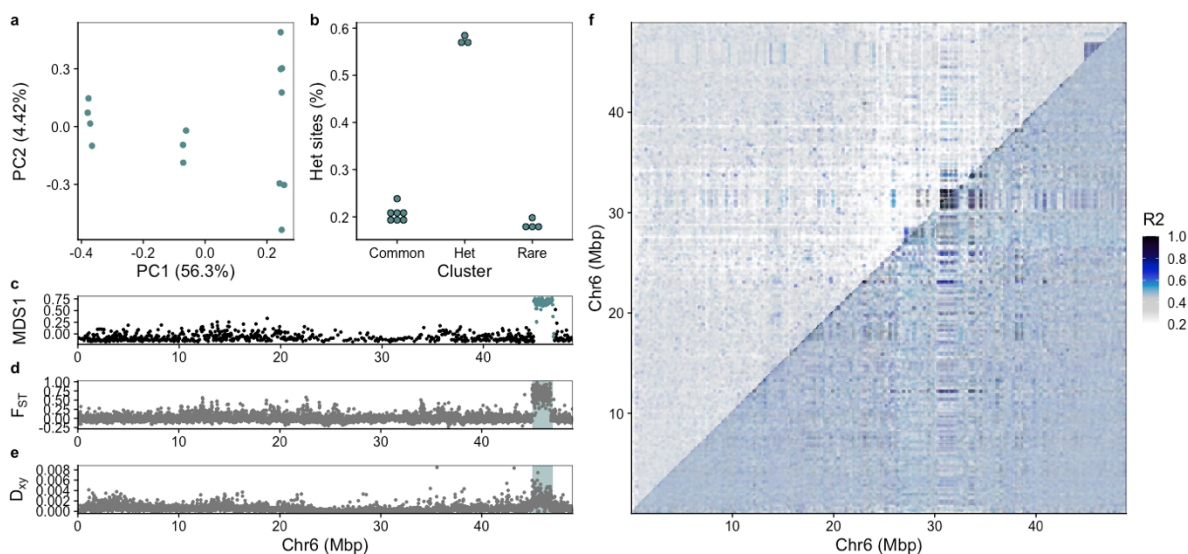
594

595 **Figure 3:** Genetic structure for Arctic cod samples (*intraspecific*) and Arctic cod vs. polar cod (*cross-*  
596 *species*) using the three different reference genomes. The map shows the different sampling localities  
597 of Arctic cod and polar cod used in this study. a, b, c) PCA of Arctic cod samples against the three  
598 references, and d, e, f) PCA of *cross-species* datasets using the three references. The three references  
599 Arctic cod, polar cod, and NEAC used for the PCAs shown below.

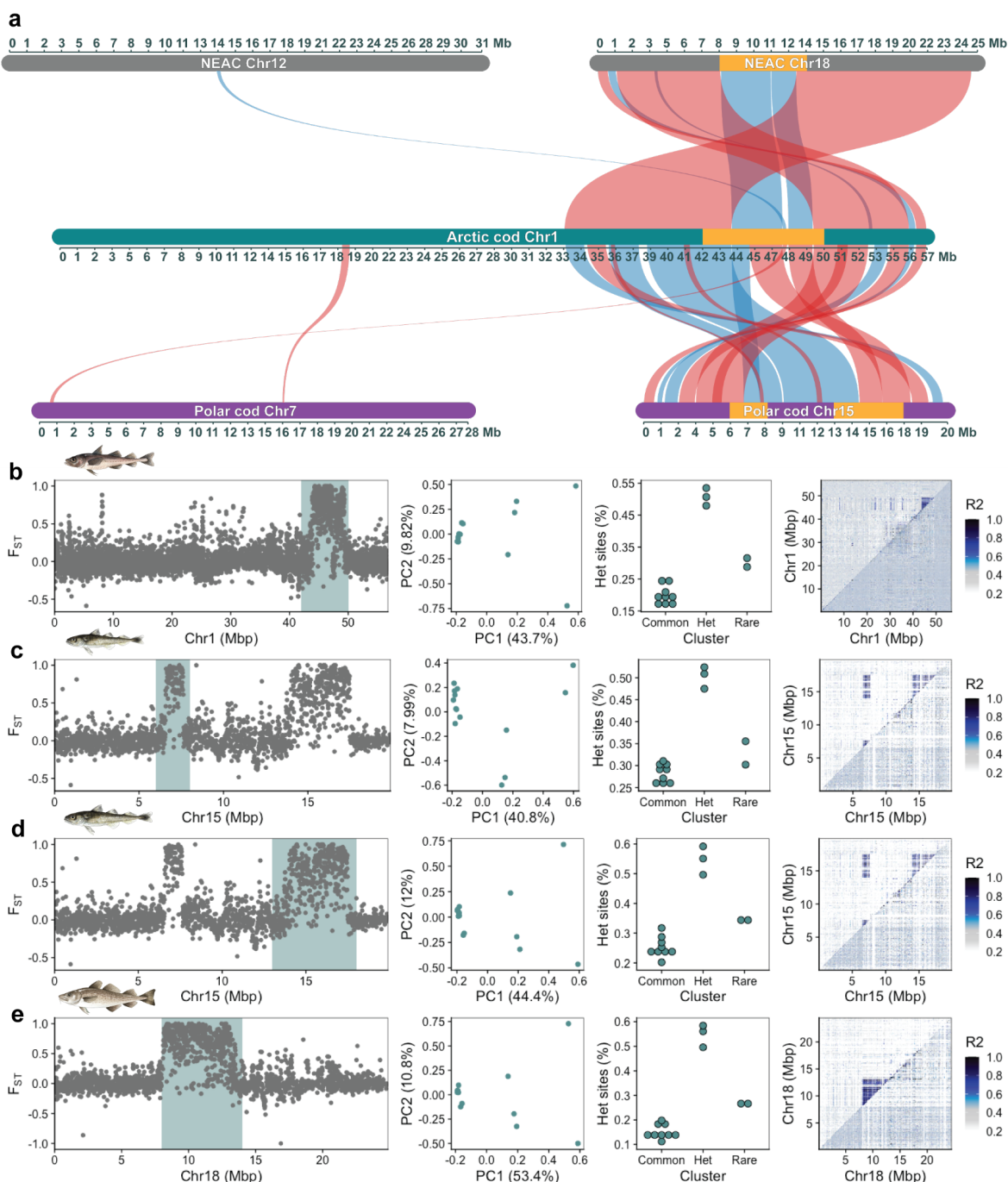
600



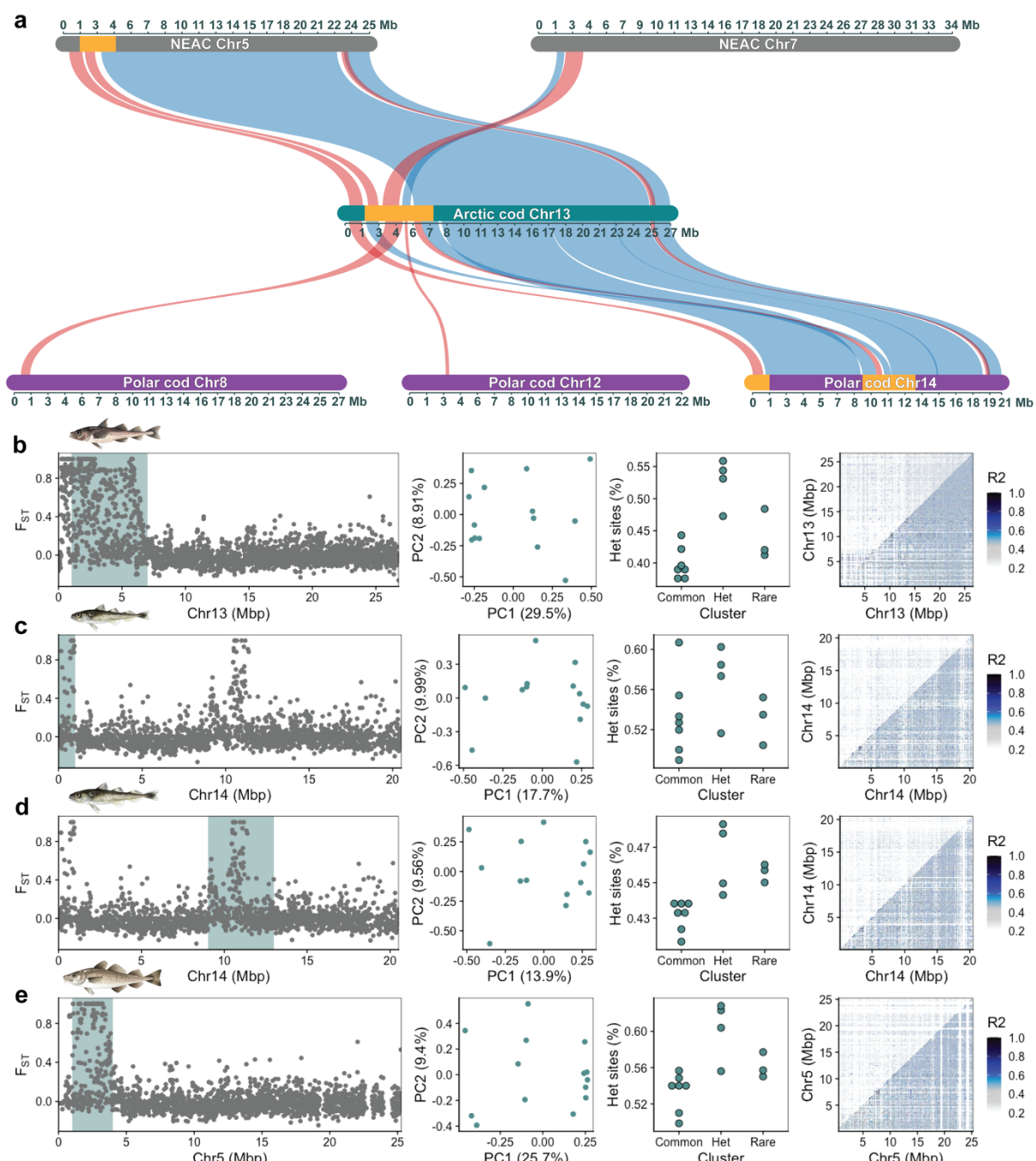
601  
602 **Figure 4:** Variability in sample statistics and population measures for the cross-species comparison  
603 using different references for Arctic cod and polar cod. a) The mean mapping depth differs for Arctic  
604 cod and polar cod samples based on the reference chosen, i.e., Arctic cod, polar cod or NEAC. The  
605 highest mean depth is seen in samples when they are mapped against their respective intraspecific  
606 references. b) Similarly, the proportion of heterozygous sites per sample, calculated using VCFtools  
607 after variant calling, also changes with the reference used. The lowest values are found in Arctic cod  
608 and polar cod when analyzed against their own intraspecific references. c) Average  $\pi$  values in windows  
609 across the three different reference genomes for each species, calculated using pixy, demonstrate  
610 variation in calculated  $\pi$  values depending on the reference used. d, f) Average  $D_{XY}$  and  $F_{ST}$  for each  
611 chromosome in the cross-species comparison of Arctic cod and polar cod, calculated using pixy, using  
612 the three different references, also show variability depending on the reference chosen.  
613  
614



615  
616 **Figure 5:** Example of how a chromosomal inversion was detected using chromosome 6 of Arctic cod  
617 as reference. a) PCA for the inversion region identified using lostruct. b) Manually assigned cluster  
618 groups and heterozygous sites given in bins for the clusters. c) MDS analysis produced by lostruct where  
619 the inversion region is highlighted. d)  $F_{ST}$  and e)  $D_{XY}$  calculated with pixy showing elevated values  
620 within the highlighted inversion region. f) pairwise linkage disequilibrium plot calculated using pixy  
621 where the top triangle includes all samples, and the lower triangle includes only the individuals within  
622 the common type. The upper right corner of the top triangle shows elevated R2 values; however, the  
623 bottom triangle, containing only individuals with homokaryotypes of the common type, does not display  
624 elevated R2 values. This pattern is in line with what is expected for a chromosomal inversion.  
625



626  
627 **Figure 6:** Example of inversion detection bias for the inversion on chromosome 1 in Arctic cod using  
628 Arctic cod, polar cod, and NEAC as reference genomes independently. a) Synvisio plots illustrating the  
629 structural rearrangements occurring between the three species' reference genomes for the second half  
630 of the Arctic cod chromosome 1; blue indicates the same orientation, while red indicates the reverse  
631 orientation, and orange indicates regions defined for the inversion detection protocol. b) Inversion  
632 detection when using Arctic cod as a reference. c) and d) Inversion detection when using polar cod as  
633 a reference, where the inversion is split into two parts that are linked together. e) When using NEAC as  
634 a reference, the inversion is successfully captured. However, a smaller part is missing, as it has  
635 translocated to chromosome 12 in NEAC. Each panel is described in further detail in Figure 5.  
636  
637



638

639

640

641

642

643

644

645

646

647

648

**Figure 7:** Example of inversion detection bias for the inversion on chromosome 13 in Arctic cod using Arctic cod, polar cod, and NEAC as reference genomes independently. a) Synvisio plots illustrating the structural rearrangements between the three species' reference genomes for Arctic cod chromosome 13, annotated with the same colors as those used in Figure 5. Here, multiple structural rearrangements between the species obscure the inversion signal for chromosome 13. b) Inversion detection using Arctic cod as a reference. c) and d) Inversion detection using polar cod as a reference, where the inversion appears as two distinct parts. Moreover, the heterozygosity signal is weaker in c), and none of the LD plots capture the inversion when using polar cod as reference. e) The inversion exhibits the expected heterozygosity distribution when using NEAC as a reference, but the LD signal is weak. Each panel is described in further detail in Figure 5.